PHYSICAL REVIEW A VOLUME 25, NUMBER 2 FEBRUARY 1982

Amplification, current-voltage variations, and refraction in the interaction between millimeter-wave radiation and the glow-discharge plasma

A. Rosenberg, Y. Ben-Aryeh, J. Politch, and J. Felsteiner
Department of Physics, Technion-Israel Institute of Technology, Haifa, Israel
(Received 3 March 1981)

The amplification of millimeter electromagnetic radiation within the cathode region of a cold-cathode glow discharge is correlated with the variations in the current-voltage characteristic of the glow discharge. The transfer of energy from the fast electrons to the electromagnetic wave amplifies the incident radiation and also causes a decrease in discharge current. The latter is called the "negative response." This negative response is superimposed on a "positive response"; i.e., an increase in current and decrease in voltage, which follows from the reduction of electron-ion recombination rate by the incident electromagnetic radiation. The negative response was extracted from the measured current-voltage variations, and the measured amplification is shown to be proportional to the negative-response voltage multiplied by the electron density. Divergence of the incident electromagnetic wave by the plasma (whose refraction index is smaller than one) was measured and compared with the theory. The effect of this divergence on the measurement of amplification is discussed. The theory of stimulated emission of bremsstrahlung has been developed to explain the above experiments. Two methods of calculations are compared: one based on differences in populations of levels, as is conventional in laser physics, and the second method which exploits the dependence of the scattering cross section on the incident electron energy. Possible improvements of the theory are discussed.

I. INTRODUCTION

Recently we reported[1] the observations of amplification of millimeter-wave radiation by stimulated emission of bremsstrahlung from the electrons in the cathode region of a cold-cathode glow discharge. Small changes in the discharge current, resulting from the incident electromagnetic (em) radiation were also reported. We claimed that the current decrease was due to the loss of electron energy to the radiation field. Therefore, this effect should occur in those discharge regions where amplification exists. However, the incident electromagnetic waves reduce the electron-ion recombination rate, which results in a current increase. This effect is responsible for the difference between the amplification curve and the current-change curve. In this paper we present a more detailed experimental and theoretical study in which amplification and current-voltage change are shown to be correlated. The refraction of the electromagnetic wave in the plasma and its effect on the measurements of amplification are also investigated. The experimental system is described in Sec. II.

The study of the current-voltage variations in the discharge caused by the incident em wave is described in Sec. III. The experimental results obtained by our group are presented and compared with previous results of other investigators. A simple model is suggested, which fits well with the experimental data, and which extracts the effect related to amplification from the measurements of the current-voltage variations.

The refraction of the incident em wave by the glow-discharge plasma is examined in Sec. IV. It is shown that the plasma diverges the incident beam as expected from the known theory. The problems in the measurements of the amplification caused by this divergence are discussed in Sec. V. In the same section the amplification is correlated with the current-voltage changes. The approximate relative electron density along the discharge tube was derived from current-voltage measurements as well as from the refraction measurements, and applied for the comparison between the amplification and the current-voltage effects.

In Sec. VI we present a detailed theoretical study of the stimulated emission of bremsstrahlung. Using the classical approximation we have compared two methods of calculation, and show that they lead to the same result for isotropic distributions. We have also discussed how the applied approximation affects the theory and how it compares with experiments.

II. EXPERIMENTAL DETAILS

The experimental system is described in Fig. 1. An electromagnetic wave at a frequency of 70 GHz (wavelength 4.3 mm) and power of 70 mW was generated by an IMPATT diode. This radiation was modulated at 833 Hz by an electronic modulator, and carried in a standard E-band rectangular wave guide to a horn. The electromagnetic wave radiated from the horn was concentrated by a lens placed close to the horn. The discharge tube was a glass cylinder, with an inside dia-

 © 1982 The American Physical Society

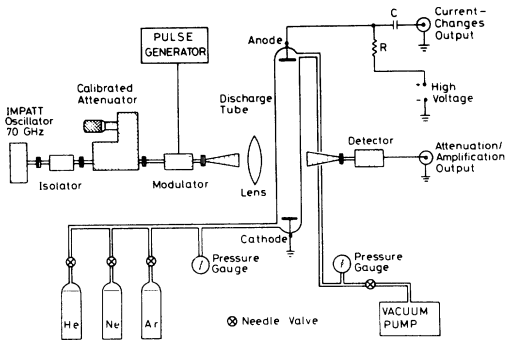

FIG. 1. Schematic diagram of the experimental system.

meter of 20 mm. Its inlet and outlet connections were connected to the vacuum pump and to the gas filling system. The electrodes were made of aluminum and were fixed at the ends of the glass cylinder, 90-mm apart. The discharge tube was placed with its axis perpendicular to the direction of propagation of the electromagnetic radiation, and in such a distance from the lens that approximately maximum concentration of the radiation was on the tube axis. The tube was movable along its axis with respect to the incident electromagnetic radiation to enable measurement at different zones of the discharge tube. The distance from the cathode to the point on the tube axis where the incident electromagnetic radiation is concentrated, is defined as X. In the present experiments the polarization of the electromagnetic wave was parallel to the tube axis.

The discharge tube was connected to the electric circuit as described in Fig. 2. V_s is the dc supply voltage, V is the voltage on the discharge tube, I is the current through the tube, $V_R = IR$ is the voltage on the resistor R. The voltage changes

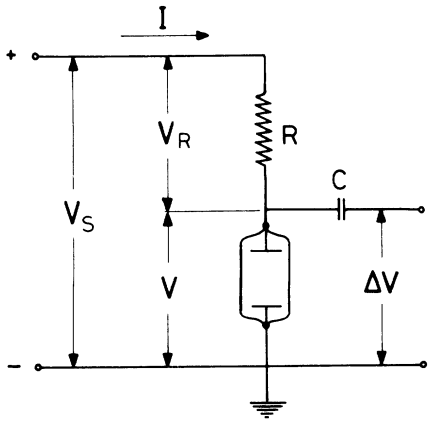

FIG. 2. Electric circuit connected to the glow-discharge tube.

ΔV in the discharge tube were separated by the capacitor C from the dc voltage V. We measured the voltage variation resulting from the em wave radiation at the modulation frequency, after filtering by a lock-in amplifier. The current change ΔI is calculated by $\Delta I = -\Delta V/R$. The minus sign indicates that an increase in current means a decrease in voltage, and vice versa.

The electromagnetic radiation crossing the tube was measured either by a crystal detector connected after a horn placed behind the glass tube, or by a point detector. Since refraction effects have influence on the measurements, the discussion of these measurements will be postponed to Sec. IV.

III. CURRENT-VOLTAGE VARIATIONS

A. Survey of previous works

The fact that the discharge current varies when the discharge tube is irradiated with electromagnetic waves in the microwave range was first reported by Burrough and Bronwell[2] about thirty years ago. It was suggested that this effect could be used for the detection of microwave radiation. The discharge tube was expected to be superior to the conventional crystal detector, and it stimulated further work on this subject.

Detailed lists of references can be found in the papers by Severin[3] and by Kopeika and Farhat.[4] Most of the works concentrated on technical aspects, such as the properties of the discharge tube as a detector. In these works the whole tube was irradiated, so that its response was some average of the responses from the various zones of the glow discharge. Obviously, for a good understanding of the current changes, one should know the separate responses in every zone of the glow discharge. Only in a few papers the current changes were measured as a function of the irradiated zone. Lampert and White[5] reported such measurements in Ne and Xe which were irradiated by a 6-cm em wave. Udelson[6] reported experiments in H_2 with 10-cm electromagnetic radiation. In these experiments the discharge tube was inserted into a special waveguide, which concentrated the radiation to a small region of the discharge. In both papers the following results were found: a current increase when the negative glow zone was irradiated, a current decrease when the Faraday dark space was irradiated, and a small current increase when the positive column was irradiated. Similar results were also reported by Bloyet and Talsky.[7]

Various models[3-12] were suggested to explain these current variations. These models will be examined later in the light of our experiments.

B. The discharge tube in the electric circuit

A cold-cathode discharge tube has a voltage versus current characteristic which depends on the geometric structure of the tube. For a cylindrical tube with plane-parallel electrodes, three main regions can be noticed[13]: (1) the dark discharge—at very low currents, (2) the glow discharge—at medium currents, and (3) the arc discharge—at very high currents.

In this work we are interested mainly in the glow discharge, which can be divided into three operating regions: (1) the subnormal region—at low currents: In this region $dV/dI<0$, therefore the discharge current is not stable and tends to oscillate. (2) the normal region—at medium currents: The cathode is only partially covered by the glow. Therefore, when the current increases a larger area of the cathode becomes covered, but there is almost no change in the current density, the cathode fall voltage, or the cathode fall length. If the positive column is short, most of the tube voltage is the cathode fall voltage; therefore: $dV/dI\cong 0$. The discharge current in this region is not very stable and contains much noise, because the glow can move randomly on the cathode face. (3) the abnormal region—at high currents: In this region the cathode is completely covered. Therefore, the current density is proportional to the current, and the voltage rises slowly with current, so that $dV/dI>0$. In this region the noise in the current is low, current densities are high, and therefore our main interest is in this region.

The tube characteristic, together with source voltage V_s and resistor R, define the working point (V and I) as described schematically in Fig. 3. The symbols in this figure refer to Fig. 2. The incident electromagnetic radiation changes the voltage-current characteristic of the tube, as described by the broken line in Fig. 3. Therefore, a new working point is defined by $V+\Delta V$ and $I+\Delta I$. ΔV is the voltage change measured as described in Fig. 2, and $\Delta I=-\Delta V/R$ is the current change to which the various workers referred. The sign of ΔV is the opposite of ΔI; although we shall refer later to voltage variations, for keeping the convention of previous works we shall use the following definitions for the response of the discharge tube to the incident electromagnetic radiation.

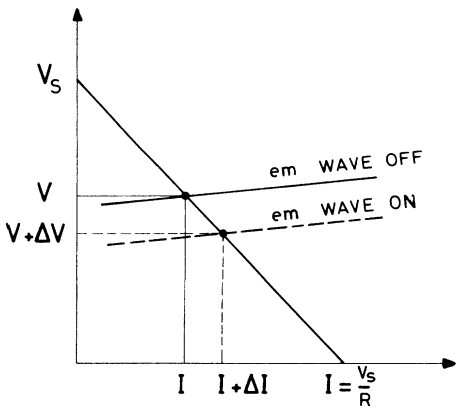

FIG. 3. Effect of the incident em wave on the working point of the glow-discharge tube.

(a) *Positive response:* $\Delta I>0$, $\Delta V<0$. The current increases, and the characteristic "moves down" on the V-I plane.

(b) *Negative response:* $\Delta I<0$, $\Delta V>0$. The current decreases, and the characteristic "moves up" on the V-I plane.

For further analysis it will be more convenient to define the following circuit-independent quantities.

(1) δV is the voltage change on the tube electrodes, due to the incident radiation, for fixed discharge current I.

(2) δI is the discharge current change, due to the incident radiation, for fixed voltage V on the electrodes.

δV and δI can be calculated from the measured value of ΔV if one knows the characteristic $V(I)$. Assuming that $\Delta V/V\ll 1$, and $\Delta I/I\ll 1$, so that the characteristic moves almost parallel to itself, one easily gets the following result:

$$\delta V=\left(1+R^{-1}\frac{dV}{dI}\right)\Delta V, \tag{1a}$$

$$\delta I=\left[1+R\left(\frac{dV}{dI}\right)^{-1}\right]\Delta I. \tag{1b}$$

We have found it more convenient to apply δV in the present work. In the experimental conditions of this work $(1/R)dV/dI$ was found to be about 0.2, so that δV is quite close to ΔV, but δI is about five times ΔI. (It should be remembered that $\delta V>0$ corresponds to "negative response," i.e., to "current decrease" in the historical terminology.)

C. Experimental results for voltage-current variations

The voltage variations at constant current δV resulting from the incident millimeter-wave radiation were measured versus X, the distance from the cathode to the irradiated zone. Results with Ne, at a pressure of 1 mm Hg, for several currents are presented in Fig. 4. At high currents, from $I=4$ mA [in Fig. 4(c)] to $I=10$ mA [in Fig. 4(f)], the results agree with the previous measurements of Lampert and White[5] and of Udelson.[6] A positive response ($\delta V<0$, $\delta I>0$) is evident at

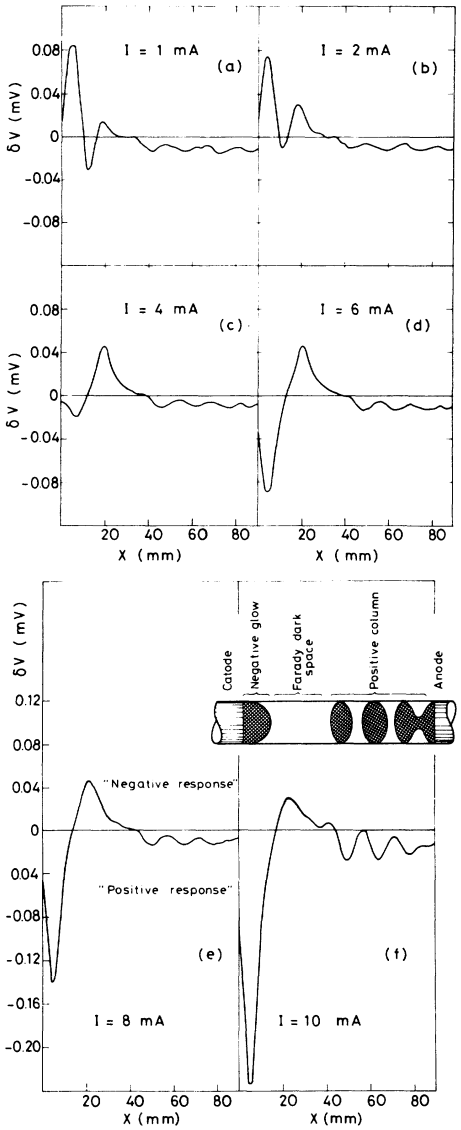

FIG. 4. Voltage variations at constant current, resulting from the incident em wave versus the distance X from the cathode. Gas: Ne pressure of 1 mm Hg. (a) $I=1$ mA, (b) $I=2$ mA, (c) $I=4$ mA, (d) $I=6$ mA, (e) $I=8$ mA, (f) $I=10$ mA. Also contains a drawing of the discharge regions.

the negative glow zone and the positive column, and a negative response ($\delta V>0$, $\delta I<0$) at the Faraday dark space. However, we have found that in the positive column the response was large when the glowing striations were irradiated, and very small when the dark striations were irradiated by the millimeter em waves. This can be seen very cleary in Fig. 4(f). At low currents a new phenomena appears: the response in the negative glow becomes negative, as can be seen in Fig. 4(b) ($I=2$ mA) and Fig. 4(a) ($I=1$ mA). However, no

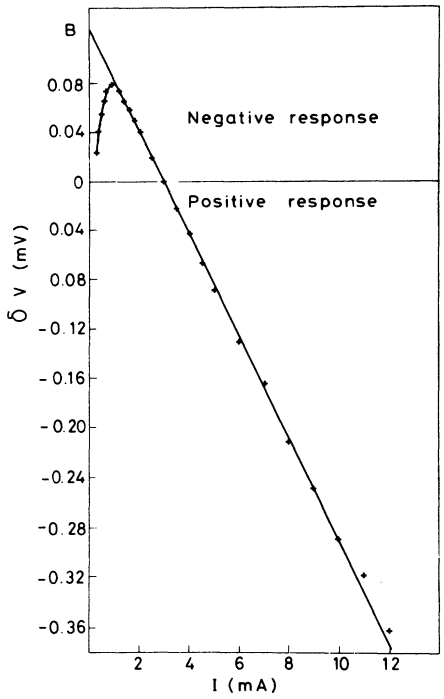

FIG. 5. Voltage variations resulting from the incident em wave versus the discharge current I. Gas: Ne, pressure of 1 mm Hg. Cathode distance: $X=7$ mm.

negative response was found in the positive column. Similar results were obtained with He, and also with discharge tubes of smaller diameter.

From the results described in Fig. 4 it is clear that the effect leading to negative response exists in the whole region from the cathode to the beginning of the positive column, and is not restricted to the Faraday dark space as has been thought earlier.[4] The positive response is connected with the glowing zones, i.e., the negative glow, and the glowing striations of the positive column, and it increases with current. In the negative glow both effects are large. The measured δV is the sum of both effects, i.e.,

$$\delta V=\delta V_B+\delta V_A, \tag{2}$$

where $\delta V_B>0$ comes from the negative effect, and $\delta V_A<0$ comes from the positive effect. In order to separate the two effects, we measured the dependence of δV on the discharge current, I, when a fixed point in the negative glow was irradiated. A typical result is described in Fig. 5, at $X=7$ mm, for Ne. In the current range from 1 to 12 mA the experimental data closely fit the equation

$$\delta V=B-AI, \tag{3}$$

where A and B are independent of the current I. Below 1 mA the curve deviates from Eq. (3) and can be approximately described by the equation

$$\delta V = B_1 - A_1/I \,. \tag{4}$$

Deviation from Eq. (3) was also found at currents above about 15 mA. It should be mentioned that at the experimental conditions described earlier (a 20-mm diameter tube with aluminum electrodes filled with Ne, to a pressure of 1 mm Hg) for currents below about 1 mA the discharge was at the normal condition. In the current range from 1 to 15 mA the discharge was at the abnormal conditions. Above 15 mA, the cathode became hot, and the discharge tends to the arc conditions.

D. Theoretical model for the current-voltage variations

Several investigators[7-11] pointed out that the positive response resulted from the decrease in electron-ion recombination rate due to the increase in the energy of the slow electrons caused by the incident em wave. This explanation is supported by the following experimental results.

(1) The response is positive in the glowing zones as can be seen in Fig. 4. At the pressure of the preceding experiments most of the recombinations end with the emission of visible light. Much of the glow of the discharge comes from this process.

(2) Quenching of spectral lines resulting from incident microwave radiation was observed in the afterglow of electric discharge in gases,[8,9,14] and in the negative glow of a glow discharge.[3,10,15] This phenomenon was explained by the reduction of recombination rate when the slow electrons absorb energy from the incident em wave, and was used in measurements of recombination rates.[16]

(3) Experiments in magnetic field[17,18] showed a resonant increase in the positive response of a glow-discharge tube at the cyclotron resonance conditions. The results were explained successfully assuming that the slow electrons absorbed energy from the em wave, and this absorption was enhanced at the cyclotron resonance.

(4) The dependence of the response on the discharge current fits well with the model based on recombination, which is presented later in this section .

In an ionization process an ion and an electron are created. The new electron is accelerated by the electric fields towards the anode. The new ion is accelerated towards the cathode, hits it, and liberates few electrons. Therefore, an increase in ionization rate increases the current and decreases the voltage, i.e., a positive response. On the other hand, in a recombination process, an ion and an electron recombine to form a neutral atom. Therefore, a decrease in recombination rate causes a current increase and voltage decrease, i.e., a positive response. The incident electromagnetic radiation may produce changes in both ionization and recombination rates, but in different ways. The ionization processes are due to fast electrons of energies above the ionization energy eV_i which is about 20 eV. As will be shown later, these fast electrons tend to lose energy to the electromagnetic wave, therefore the number of ionizations decrease and the current decreases, i.e., a negative response. The recombination process is between ions and slow electrons, whose energy is of the order of few meV—ie., thermal electrons. These slow electrons absorb energy from the electromagnetic wave, therefore, the recombination rate decreases and the current increases, i.e., a positive response.

The number of recombinations per second is given by[16]

$$R = -\left(\frac{dn_i}{dt}\right)_R = -\left(\frac{dn_e}{dt}\right)_R = \alpha_R n_i n_e^s \,, \tag{5}$$

where n_i is the ion density, n_e^s is the slow-electron (thermal electron) density, and α_R is the recombination coefficient. We shall not discuss the exact mechanism, but following Chen *et al.*,[16] the recombination coefficient reduces, due to the incident electromagnetic radiation, from α_R to $\alpha_R - \Delta\alpha_R$ ($\Delta\alpha_R > 0$). Therefore, the change in the number of recombinations per second is

$$\Delta R = -\Delta\alpha_R n_i n_e^s \,. \tag{6}$$

The electron energy before the recombination is negligible relative to the ionization energy (few meV compared to about 20 eV), therefore the energy loss from the discharge by one recombination is eV_i. The change in power loss, resulting from the incident em wave, is $eV_i\Delta R$. If the current through the tube is constant, this change in power loss should be compensated by an equal change in the power delivered to the tube by the external source. This power is $I\delta V_A$, where δV_A is the change in tube voltage. So we obtain

$$I\delta V_A = eV_i\Delta R = -eV_i\Delta\alpha_R n_i n_e^s \,, \tag{7}$$

eV_i and $\Delta\alpha_R$ are independent of the discharge current I. In the abnormal range, the current density is proportional to the current, therefore both n_e^s and n_i are proportional to the current I. Therefore,

$$n_i n_e^s = \gamma I^2 \,, \tag{8}$$

where γ is some proportionality constant, which depends on the discharge structure. With Eqs. (7) and (8) we obtain

$$\delta V_A = -(eV_i\Delta\alpha_R\gamma)I \,. \tag{9}$$

This last equation explains the positive response terms $-AI$ appearing in Eq. (3), which was derived

from our experimental data. We identify

$$A = eV_i \Delta\alpha_R \gamma . \tag{10}$$

Deviations from Eq. (9) appear whenever Eq. (8) fails. At the normal operating range (below about 1 mA at our experimental conditions) the current density near the cathode is almost constant (independent of the current), therefore n_e^s and n_i are independent of the current I. From Eq. (7) we get

$$\delta V_A = -eV_i \Delta\alpha_R n_i n_e^s / I , \tag{11}$$

which explains the positive response term in Eq. (4), with the identification

$$A_1 = eV_i \Delta\alpha_R n_i n_e^s . \tag{12}$$

At high currents, the discharge tends to the arc conditions, therefore a deviation from Eq. (3) was found.

The negative response, i.e., decrease in current and increase in voltage, was defined as δV_B in Eq. (2), and equals the term B in Eq. (3), which was derived from the experimental data. We have already suggested[1] that the negative response follows from the stimulated emission of bremsstrahlung by the fast electrons, and therefore relates to the amplification. In the collision process between a free electron and an atom (or molecule) in the presence of an electromagnetic wave, energy is exchanged between the em wave and the electron.[19,20] As we shall show in Sec. VI, for a distribution of fast electrons, energy is transferred from the electrons to the electromagnetic wave. One result is the amplification of the em wave described in Sec. V; another result is the decrease in discharge current and increase in discharge voltage, which we called negative response.

The analysis presented in this section can be applied to extract the negative-response voltage δV_B, from the current-voltage measurements. The voltage change ΔV is measured as a function of the discharge current I, δV is calculated with Eq. (1a) from ΔV, and plotted as a function of I as was done in Fig. 5; the coefficients A and B in Eq. (3) are chosen to give the best fit of that equation with the linear portion of the graph. B is the negative-response voltage δV_B which we shall correlate with the amplification. In the Faraday zone, where the recombination effect is low, the positive response is negligible and the measured δV is exactly the negative-response voltage δV_B.

IV. REFRACTION OF THE ELECTROMAGNETIC WAVE IN THE PLASMA

The refraction of the electromagnetic wave in the plasma has the important implications on the measurements and applications of the amplification effect. Electrons and ions in conditions of quasineutrality create the plasma state. Many phenomena in plasma are explained by the Coulomb forces alone, neglecting the collisions between electrons and ions. In the glow discharge the gas is only partially ionized: about one electron-ion pair per 10^4 neutral atoms. The neutral atoms do not disturb the Coulomb forces. Therefore, if the electron–neutral-atom collision frequency is not too high, some plasma properties of the glow discharge can be described neglecting the neutral atoms. One of these properties is the propagation and refraction of the electromagnetic wave in the discharge. On the other hand, the presence of neutral atoms is responsible for the stimulated emission of bremsstrahlung radiation, which amplifies the incident electromagnetic wave. In the glow discharge, at our experimental conditions, both refraction and amplification of the incident wave take place simultaneously.

The propagation of electromagnetic waves in plasma is discussed by Chen.[21] The dispersion relation is given by

$$\omega^2 = \omega_P^2 + c^2 k^2 , \tag{13}$$

where ω and $\vec{k}$ are the incident wave frequency and wave vector, respectively, ω_P is the plasma frequency defined by

$$\omega_P^2 = \frac{4\pi e^2 n_e}{m} . \tag{14}$$

The refraction index N is given by

$$N = \frac{ck}{\omega} = \left(1 - \frac{\omega_P^2}{\omega^2}\right)^{1/2} . \tag{15}$$

For $\omega_P > \omega$, N is imaginary, and the electromagnetic wave cannot propagate through the plasma. For $\omega_P < \omega$, N is real and smaller than one. In our experiments ω is constant and n_e varies. Therefore we define

$$n^0 \equiv \frac{m}{4\pi e^2}\omega^2 \cong 6\times 10^{13}, \tag{16}$$

where n^0 is in cm^{-3}.

Then the dependence of N on n_e becomes

$$N = \left(1 - \frac{n_e}{n^0}\right)^{1/2} \cong \left(1 - \frac{n_e}{6\times 10^{13}}\right)^{1/2} \tag{17}$$

and for small n_e (compared to n^0),

$$N \cong 1 - \frac{n_e}{2n^0} . \tag{18}$$

For $n_e = 10^{13}$, $N = 0.91$. In order to get N significantly different from one, n_e must be very close to $n^0 \cong 6\times 10^{13}$ cm^{-3} (for a frequency of 70 GHz).

The significance of a refraction index smaller than one was pointed out by Chen.[21] A plasma in the shape of a convex lens diverges the incident electromagnetic wave. In our system the incident em wave is expected to be diverged in the following way.

(1) Since the tube is cylindrical, the plasma has this shape, so the wave diverges as described schematically in Fig. 6. In the left-hand side of the figure the expected variations in radiation intensity behind the tube were drawn. Y and W are defined in Fig. 8.

(2) The electron density changes along the tube axis. According to known literature,[13] the electron density is maximal in the middle of the negative glow, and decreases towards the positive column. Therefore, we expect the incident wave to be affected by the plasma as described in Fig. 7.

When measuring amplification, the refraction of the incident wave by the plasma should be considered, since both effects change the intensity at every point behind the tube. This problem can be overcome by placing a collecting horn with a large aperature close to the tube (Fig. 1), so that most of the radiation crossing the tube will reach the detector. However, when the electron density is very close to $n^0 = 6\times10^{13}$ cm^{-3}, the incident wave is refracted strongly by the plasma, and the power reaching the detector decreases.

Measurements of the refraction were proceeded with the system described in Fig. 1, with the arrangement described in Fig. 8 replacing the collecting horn. The intensity variations were measured in the W-Y plane defined in Fig. 8. The millimeter-wave detector was a miniature glow-discharge tube, of type PFE 455, whose detection properties had been studied.[17,18,22,23] This tube responds to the radiation falling on its negative glow, whose diameter is about 2 mm. The detector

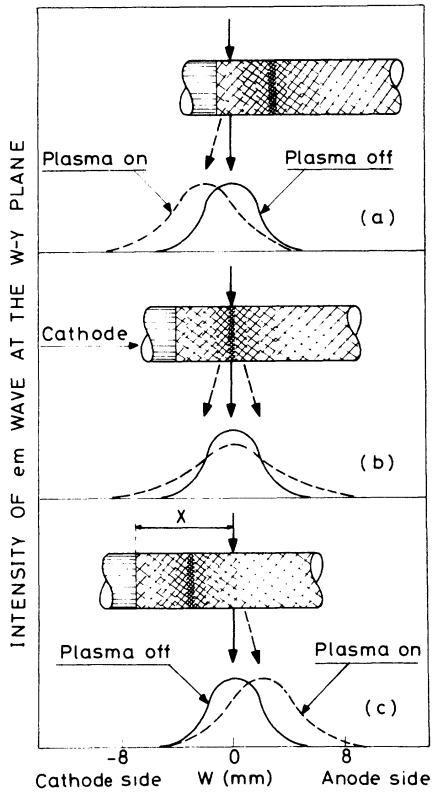

FIG. 7. Schematic description of the expected divergence of the em wave by the plasma, in the W direction: (a) for em wave incident close to the cathode, (b) for em wave incident into the region of maximum electron density, and (c) for em wave incident close to the Faraday region.

was moved in the W-Y plane, in a square of 24×24 mm^2 centered at $W=0$, $Y=0$, and changes in detected signal caused by the discharge were measured in spacing of 4 mm. The measurements were repeated for various values of cathode distance X, from $X=2$ to $X=20$ mm.

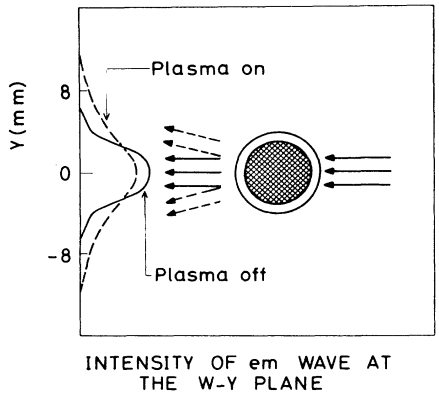

FIG. 6. Schematic description of the expected divergence of the em wave by the plasma, in the Y direction.

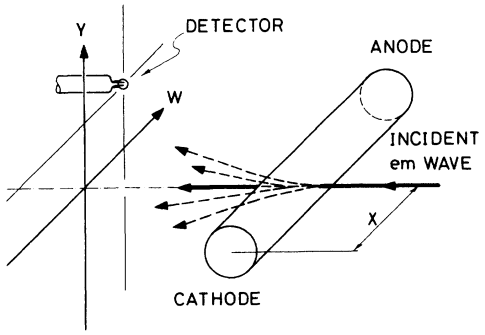

FIG. 8. Schematic diagram of the experimental arrangement for measuring the divergence of the em wave by the plasma.

The measurements were made with Ne, at a pressure of 1 mm Hg, and discharge current of 10 mA. The results were in agreement with the qualitative predictions described in Figs. 6 and 7. To demonstrate this, we summed in the W direction for X constant, and got the intensity variations as functions of Y. These intensity variations were plotted in Fig. 9 for several values of X. These curves are in good agreement with the prediction in Fig. 6. The curve in Fig. 9 does not go below zero for $Y=0$ because the amplification effect is superimposed on the refraction effect, and shifts the curves "upwards."

Summation in the Y direction for X constant yielded the intensity variations as functions of W. These intensity variations were plotted in Fig. 10 for several values of X. $X=2$ and $X=4$ mm correspond to the prediction in Fig. 7(a), $X=6$ mm corresponds to Fig. 7(b), and $X=8$ and $X=10$ mm to Fig. 7(c).

V. AMPLIFICATION

A. Amplification and current-voltage variations

The current-voltage-variation effect, which was described in Sec. III, is composed to two opposite effects. The positive one, caused by the decrease in recombination is not related to the amplification because the energy absorption by the slow (thermal) electrons is very small. The negative effect caused by the transfer of energy from the fast electrons to the electromagnetic wave is related to the amplification phenomena. The analysis presented in Sec. III enabled us to derive the negative response voltage δV_B from the experimental data. δV_B is proportional to the energy loss of the fast electrons but independent of the current I, i.e., independent of the electron density n_e. The amplification h is proportional to the energy loss of the fast electrons and to the fast-electron density n_e^F. Therefore, we expect

$$h \sim n_e^F \delta V_B . \tag{19}$$

The quantities h, n_e, and δV_B vary as functions of the cathode distance X. The amplification $h(X)$ was measured directly with a horn and a crystal detector as described in Fig. 1.

Evaluation of $n_e^F(X)$ is somewhat more complicated. We assume that the fast-electron density $n_e^F(X)$ is proportional to the slow-electron density $n_e^S(X)$, and to the total electron density $n_e(X)$. The dependence of n_e^S on X can be derived from the X dependence of the coefficient A in Eq. (3), so it can be evaluated from the current-voltage measurements reported in Sec. III. The X dependence of the total electron density can be evaluated from the refraction measurements of Sec. IV. According to Eq. (18) the deviation of the refraction index N from one is proportional to n_e in the first approximation. Since the divergence of the em wave is proportional to the deviation of N from one, it is also proportional to n_e.

Results with Ne at a pressure of 1.0 mm Hg and current of 10 mA are presented in Fig. 11. In part (a) the normalized electron densities are described as functions of X. The full line is the

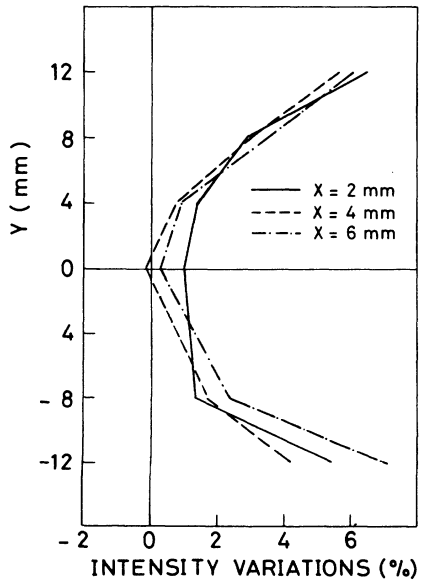

FIG. 9. Measured intensity variations of the em wave, caused by the plasma, in the Y direction. Gas: Ne, 1-mm Hg pressure, $I=10$ mA.

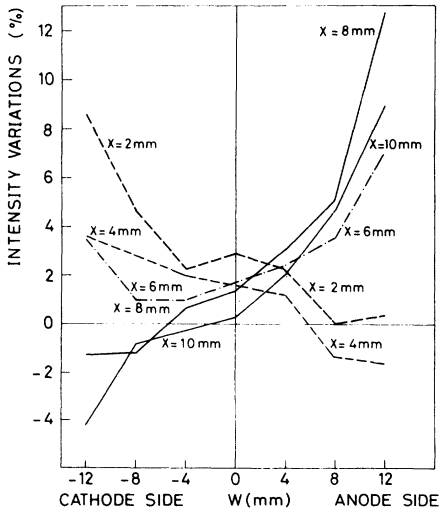

FIG. 10. Measured intensity variations of the em wave caused by the plasma in the W direction. Gas: Ne, 1-mm Hg pressure, $I=10$ mA.

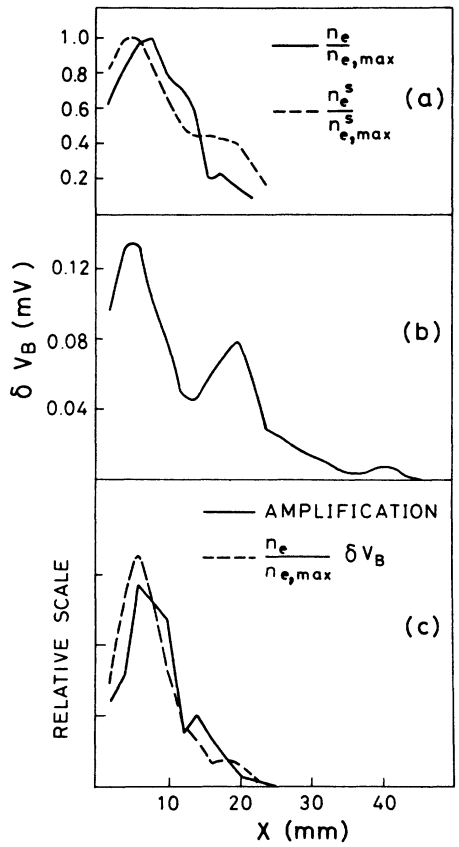

FIG. 11. (a) Normalized electron densities versus cathode distance X. Full line: derived from the refraction measurements. Dashed line: derived from the voltage variations measurements. (b) Negative-response voltage versus cathode distance X. (c) Comparison between the amplification (full line) and the negative-response voltage multiplied by the normalized electron density (dashed line). Gas: Ne, 1-mm Hg pressure, $I = 10$ mA.

total density $n_e(X)/n_{e,\max}$ evaluated from refraction measurements. The dashed line is the slow-electron density $n_e^S(X)/n_{e,\max}^S$ derived from the coefficient A. In part (b) the negative response $\delta V_B(X)$ was drawn. In part (c) the amplification $h(X)$ was drawn in full line and compared with $[n_e(X)/n_{e,\max}] \times \delta V_B$ calculated from parts (a) and (b), and drawn in dashed lines. The scales are relative since we wish to demonstrate that the two quantities are proportional. The results presented in Fig. 11(c) agree with the expectation of Eq. (19), and confirm the statement that the amplification and the negative response are correlated.

B. Amplification and refraction

As we noted in Sec. IV the refraction of the incident em wave by the plasma should be taken into account when measuring amplification. To evaluate this effect in the present measurements, we calculated the amplification from the intensity variations measured as described in Fig. 8 of Sec. IV. The intensity variations were summed in the W-Y plane, and we obtained the amplification as function of X. This result was compared with a measurement done with a horn close to the discharge tube. In the region of high electron density, where the divergence of the incident em was large, the amplification measured with the horn was greater than that measured in the W-Y plane. That difference follows from the greater collecting area of the horn. In the regions of lower electron density the two measurements yielded the same result.

C. Amplification versus the incident power

The amplification was measured as a function of the incident power, in the conditions described earlier, at the region of maximum amplification, i.e., $X = 6$ mm. The millimeter-wave-radiation power reaching the discharge tube was approximately 10 mW. When it was attenuated by 40 dB, i.e., the power reduced by a factor of 10^4, no significant change was found in the amplification. This independence of the incident power is characteristic in stimulated emission processes, and is derived theoretically for the bremsstrahlung process in Sec. VI.

VI. THEORY OF AMPLIFICATION BY STIMULATED EMISSION OF BREMSSTRAHLUNG

A. Introduction

The possibility of amplification of electromagnetic wave by stimulated emission of bremsstrahlung was suggested in 1962 by Marcuse.[24] He calculated the emission cross section for electrons scattered by the Coulomb potential. According to his calculations, ion density of a solid was required for a reasonable amplification, therefore he suggested using an electron beam scattered on a solid. Other authors used the principle of "integral detailed balancing" to calculate the emission cross section. Reviews of these subjects can be found in a paper by Bunkin *et al.*[25] and by Federov[26].

The development of high-power lasers raised interest in the subject of charged particle scattering in the presence of a laser field, sometimes called "free-free radiative transitions of electrons." Kroll and Watson[27] derived theoretically the following basic equation

$$\frac{d\sigma_\nu(\vec{q}(\nu),\vec{q}_0)}{d\Omega} = \frac{q(\nu)}{q_0} J_\nu^2\left(e\frac{\vec{a}\cdot\vec{Q}}{mc\hbar\omega}\right)\frac{d\sigma_{el}(\epsilon,\vec{Q})}{d\Omega}, \qquad (20)$$

where $d\sigma_\nu(\vec{q}(\nu),\vec{q}_0)/d\Omega$ is the differential cross section for scattering from (time-averaged) initial momentum $\vec{q}_0$ to final momentum $\vec{q}(\nu)$ with the emission ($\nu>0$) or absorption ($\nu<0$) of ν photons of angular frequency ω, so that

$$\frac{q(\nu)^2}{2m}=\frac{q_0^2}{2m}-\nu\hbar\omega, \tag{21}$$

$d\sigma_{el}/d\Omega$ is the differential elastic scattering cross section for scattering in the absence of the electromagnetic field, evaluated at energy ϵ and momentum transfer

$$\vec{Q}\equiv\vec{q}(\nu)-\vec{q}_0. \tag{22}$$

The electric field direction is denoted by $\hat{a}$, $\vec{a}$ is the vector potential of the plane wave. J_ν is the Bessel function of order ν.

Equation (20) had been suggested for low frequencies, but was derived later in many different ways, under various assumptions. Its experimental verification was reported by Weingartshofer *et al.*,[19,20] and by others. A review of Gavrila and Van der Wiel[28] was published in 1978, but many more experimental and theoretical works on these subject have been published recently.[29] Most of the investigators were interested in scattered-electron spectroscopy and its applications for studying atomic and molecular structures.

The great importance of laser fusion initiated research on absorption of energy by the plasma from the laser field through the mechanism of inverse bremsstrahlung absorption. The calculations were done[30] for Maxwellian and other electron distributions, which were expected to exist in high-temperature plasmas. For such distributions it was found that energy is transferred from the electromagnetic wave to the plasma.

In this section a theory of stimulated emission of bremsstrahlung will be presented in a form suitable for explaining the amplification. Two methods of calculations will be used. One method is based on the conventional physical approach to laser physics, i.e., the differences in population of levels are calculated. This method is also used for calculating laser energy absorption in plasma.[30] In the second method, the dependence of the scattering cross section on the incident electron energy is considered. Our result derived classically becomes equal to the one derived quantum mechanically by Mittleman.[31] Expressions for isotropic electron distribution are derived in both methods, and are shown to be the same. Other distributions are also considered. Orders of magnitude of the amplification are calculated, and we discuss the limitations of the model and possible ways of improving the model.

B. Basic assumptions

(1) Classical calculations: The motion of the electron in the electromagnetic field is treated classically. This is allowed since according to Eq. (20) an order of one hundred photons may be emitted or absorbed in a single electron-atom collision, at our experimental conditions.

(2) Low-frequency approximation: The time of a collision is much smaller than the period of the electromagnetic wave, so that the electric field of the wave can be considered constant during the collision.

(3) Plane-wave approximation: The incident electromagnetic wave is considered as an infinite plane wave.

(4) The electric field is taken independent of position. Assumptions 3 and 4 are not too good for our experimental conditions.

(5) The collision cross section is assumed to be unaffected by the incident electromagnetic wave.

(6) The mass of the atoms is assumed to be infinite.

(7) Only elastic collisions are considered, but the model can be extended to inelastic collisions.

C. Basic equations (cgs units)

The motion of a particle with a charge e in an electromagnetic field is described by

$$\vec{p}=\vec{q}-\frac{e}{c}\vec{A}, \tag{23}$$

where $\vec{p}=m\vec{v}$ is the kinetic momentum, $\vec{q}$ is the canonical conjugate of $\vec{r}$: quantum mechanically $\vec{q}=-i\hbar\partial/\partial\vec{r}$, classically $\vec{q}$ is the time average of $\vec{p}$, $\vec{A}$ is the vector potential, and for an electron $e\equiv-|e|$. According to the assumptions, the electromagnetic field is described by

$$\vec{A}=\vec{a}\cos\omega t\equiv\vec{a}\cos\alpha. \tag{24}$$

An electron of initial momentum $\vec{q}_1$ and energy $E_1=q_1^2/2m$, enters the region of the incident em wave, and is scattered elastically at time t by an atom. The initial kinetic momentum at time t is given by

$$\vec{p}_1(t)=\vec{q}_1-\frac{e}{c}\vec{a}\cos\omega t. \tag{25}$$

The electron leaves the collision at the kinetic momentum $\vec{p}_2$. Since the collision time is much smaller than the period of the electromagnetic wave, $\vec{A}$ is assumed to be constant during the collision, so that

$$\vec{p}_2(t)=\vec{q}_2-\frac{e}{c}\vec{a}\cos\omega t\ . \tag{26}$$

If the collision is elastic the kinetic momentum

is not changed in magnitude:

$$p_2(t) = p_1(t) . \tag{27}$$

The electron leaves the em field region with energy $E_2 = q_2^2/2m$.

The energy exchange ΔE between the electron and the field can be derived from Eqs. (25)–(27),

$$\Delta E \equiv E_2 - E_1 = \frac{q_2^2}{2m} - \frac{q_1^2}{2m} = \frac{e}{mc} \vec{a} \cdot \vec{Q} \cos\omega t, \tag{28}$$

where $\vec{Q}$ is the momentum transfer, given by

$$\vec{Q} = \vec{q}_2 - \vec{q}_1 = \vec{p}_2(t) - \vec{p}_1(t) . \tag{29}$$

If $\Delta E > 0$ the electron absorbed energy from the em wave, and if $\Delta E < 0$ the energy was transferred to the em wave.

The probability of an electron making a collision is related to the collision cross section. In the low-frequency approximation, and neglecting the effect of the em wave on the collision process itself, the cross section can be taken as the cross section without the em wave, and it is a function of the initial and final kinetic momenta $\vec{p}_1(t)$ and $\vec{p}_2(t)$, i.e., $d\sigma(\vec{p}_1, \vec{p}_2)/d\Omega$.

The flux of a single incident electron is taken as $\vec{p}_1/m$. If there are n_a atoms per one cubic cm, then the transition rate of an electron scattered at time t into a solid angle $d\Omega_{p_2}$ is given by

$$dR = n_a \frac{p_1}{m} \frac{d\sigma(\vec{p}_1, \vec{p}_2)}{d\Omega} d\Omega_{p_2} . \tag{30}$$

D. Difference in population method

The solid angle $d\Omega_{p_2}$ can be expressed as follows:

$$d\Omega_{p_2} = \frac{d^3p_2}{p_2^2} \delta(p_2 - p_1) = \frac{d^3p_2}{p_2^2} 2p_2 \delta(p_2^2 - p_1^2)$$

$$= \frac{2d^3p_2}{p_2} \delta(p_2^2 - p_1^2), \tag{31}$$

where a known property of the δ function was used. From Eqs. (25) and (26) we get

$$p_2^2 - p_1^2 = q_2^2 - q_1^2 - 2\frac{e}{c} \vec{a} \cdot \vec{Q} \cos\alpha , \tag{32}$$

where $\alpha \equiv \omega t$. Therefore,

$$d\Omega_{p_2} = \frac{2d^3q_2}{p_2} \delta\left(q_2^2 - q_1^2 - 2\frac{e}{c} \vec{a} \cdot \vec{Q} \cos\alpha\right) . \tag{33}$$

Substituting (33) into (30) we get

$$dR = n_a \frac{1}{m} \frac{d\sigma(\vec{p}_1, \vec{p}_2)}{d\Omega} 2\, d^3q_2 \delta\left(q_2^2 - q_1^2 - 2\frac{e}{c} \vec{a} \cdot \vec{Q} \cos\alpha\right) . \tag{34}$$

Assuming an electron distribution $f(\vec{q})$ normalized by

$$\int f(\vec{q}) d^3q = 1 , \tag{35}$$

then the number of electrons with momentum $\vec{q}$ in the range d^3q is given by $n_e f(\vec{q}) d^3q$ where n_e is the electron density (cm^{-3}). The energy absorbed per unit time per unit volume (erg cm^{-3} sec^{-1}) in the transitions from $\vec{q}_1$ to $\vec{q}_2$ at time t is

$$d\dot{W}_{1\to 2} = n_e f(\vec{q}_1) d^3q_1 \Delta E\, dR$$

$$= n_e n_a \frac{2}{m} d^3q_1 d^3q_2 f(\vec{q}_1) \left(\frac{e}{mc} \vec{a} \cdot \vec{Q} \cos\alpha\right)$$

$$\times \frac{d\sigma(\vec{p}_1, \vec{p}_2)}{d\Omega} \delta\left(q_2^2 - q_1^2 - 2\frac{e}{c} \vec{a} \cdot \vec{Q} \cos\alpha\right) , \tag{36}$$

where ΔE and dR where substituted from Eqs. (28) and (34), respectively.

In Eq. (36), $d\sigma/d\Omega$ depends on $\vec{p}_1$ and $\vec{p}_2$, which are functions of time, and therefore, of $\alpha \equiv \omega t$. Since $\Delta E \ll E_1$, we may not neglect the small dependence of $d\sigma/d\Omega$ on α and integrate over it. Also we may not neglect the small differences between the $\vec{p}$'s and the $\vec{q}$'s, since these small differences are the cause of the amplification effect. To overcome this problem the conventional method of laser physics may be used. The inverse transition from $\vec{q}_2$ to $\vec{q}_1$ is considered. The power absorbed:

$$d\dot{W}_{2\to 1} = \frac{2}{m} n_e n_a d^3q_2 d^3q_1 f(\vec{q}_2) \left(\frac{e}{m} \vec{a} \cdot \vec{Q}' \cos\alpha \ \frac{d\sigma(\vec{p}_2, \vec{p}_1)}{d\Omega}\right)$$

$$\times \delta\left(q_1^2 - q_2^2 - 2\frac{e}{c} \vec{a} \cdot \vec{Q}' \cos\alpha\right), \tag{37}$$

where $\vec{Q}' \equiv \vec{q}_1 - \vec{q}_2 = -\vec{Q}$, and combining the two transitions we get

$$d\dot{W}_{1,2} = n_e n_a \frac{2}{m} d^3q_1 d^3q_2 \left(\frac{e}{mc} \vec{a} \cdot \vec{Q} \cos\alpha\right)$$

$$\times \delta\left(q_2^2 - q_1^2 - 2\frac{e}{c} \vec{a} \cdot \vec{Q} \cos\alpha\right)$$

$$\times \left(f(\vec{q}_1) \frac{d\sigma(\vec{p}_1, \vec{p}_2)}{d\Omega} - f(\vec{q}_2) \frac{d\sigma(\vec{p}_2, \vec{p}_1)}{d\Omega}\right) . \tag{38}$$

For elastic collisions the process is symmetric, so that

$$\frac{d\sigma(\vec{p}_1, \vec{p}_2)}{d\Omega} = \frac{d\sigma(\vec{p}_2, \vec{p}_1)}{d\Omega} . \tag{39}$$

Therefore, $d\sigma/d\Omega$ can be taken out of the large parentheses in Eq. (38). $d\dot{W}_{1,2}$ of Eq. (38) should be integrated over d^3q_1 and d^3q_2, and divided by two since we count each transition twice. Also, we should average over the period of the em wave, i.e., integrate with $\int_0^\pi d\alpha/\pi$. Then the power absorbed in a unit volume is

$$\dot{W}=\frac{1}{m^2}n_e n_a\int d^3q_1\int d^3q_2\int_0^{\pi}\frac{d\alpha}{\pi}\left(\frac{e}{c}\vec{a}\cdot\vec{Q}\cos\alpha\right)\frac{d\sigma(\vec{p}_1,\vec{p}_2)}{d\Omega}[f(\vec{q}_1)-f(\vec{q}_2)]\delta\left(q_2^2-q_1^2-2\frac{e}{c}\vec{a}\cdot\vec{Q}\cos\alpha\right). \tag{40}$$

In Eq. (40) the term containing small differences is now $[f(\vec{q}_1)-f(\vec{q}_2)]$. Therefore the equation is not sensitive to small changes in the cross section $d\sigma/d\Omega$, and $d\sigma/d\Omega$ may be taken as a function of $\vec{q}_1$ and $\vec{q}_2$, or of E_1 and $\vec{Q}$.

For Maxwellian distribution of electrons, it was shown[30] that energy is absorbed by the electrons from the em wave, i.e., $\dot{W}>0$. But for other types of distributions $\dot{W}$ may be negative and the electromagnetic wave is amplified. As an example, we examined a distribution created by a beam of electrons directed initially in the X direction, and diverged by collisions. Such a distribution can be approximated by

$$f(\vec{q})=\frac{b}{\pi}f(q_x)e^{-b(q_y^2+q_z^2)}, \tag{41}$$

where b is a parameter describing the width of the distribution in the perpendicular direction. $f(q_x)$ vanishes below a certain value $q_{x,\min}$ and is supposed to be "inverted" for the lower range of q_x, i.e., $df/dq_x>0$ in this range. The distribution of (41) was substituted into Eq. (40). Then $\vec{q}_1$ and $\vec{q}_2$ were replaced by the variable $\vec{Q}$ defined in Eq. (29) and the variable $\vec{q}$ defined by

$$\vec{q}=\tfrac{1}{2}(\vec{q}_1+\vec{q}_2), \tag{42}$$

so we obtained

$$\dot{W}=\frac{1}{m^2}n_e n_a\int d^3q\int d^3Q\int_0^{\pi}\frac{d\alpha}{\pi}\frac{d\sigma}{d\Omega}\left(\frac{e}{c}\vec{a}\cdot\vec{Q}\cos\alpha\right)\delta\left(2\vec{q}\cdot\vec{Q}-2\frac{e}{c}\vec{a}\cdot\vec{Q}\cos\alpha\right)$$
$$\times\frac{b}{\pi}(f(q_x-\tfrac{1}{2}Q_x)\exp\{-b[(q_y-\tfrac{1}{2}Q_y)^2+(q_z-\tfrac{1}{2}Q_z)^2]\}$$
$$-f(q_x+\tfrac{1}{2}Q_x)\exp\{-b[(q_y+\tfrac{1}{2}Q_y)^2+(q_z+\tfrac{1}{2}Q_z)^2]\}). \tag{43}$$

For electrons of a beamlike distribution, which are scattered in the forward direction mainly, $f(q_x)$ can be approximated by

$$f(q_x\pm\tfrac{1}{2}Q_x)\cong f(q_x)\pm\frac{df(\frac{1}{2}Q_x)}{dq_x}. \tag{44}$$

After substituting Eq. (44) into Eq. (43) the integration over Q_x was performed, using the δ function; then the integral over α was evaluated. Only terms containing $\cos^2\alpha$ did not vanish in this integration. The integration over q_y and q_z was performed, assuming that $d\sigma/d\Omega$ depends on the momentum transfer Q only. Finally, we define the transverse momentum transfer Q by

$$Q^2=Q_y^2+Q_z^2 \tag{45}$$

and obtain the following results.

For em wave polarization in the X direction

$$\dot{W}=-n_e n_a\frac{1}{m^2}\frac{\pi}{8}\int_{q_{x,\min}}^{\infty}dq_x\int_0^{\infty}dQ\,Q^3\frac{1}{bq_x^4}\frac{df}{dq_x}\left(\frac{e}{c}a\right)^2\frac{d\sigma}{d\Omega} \tag{46}$$

and for polarization in the Y direction

$$\dot{W}=-n_e n_a\frac{1}{m^2}\frac{3\pi}{16}\int_{q_{x,\min}}^{\infty}dq_x\int_0^{\infty}dQ\,Q^3\frac{1}{q_x^2}\frac{df}{dq_x}\left(\frac{e}{c}a\right)^2\frac{d\sigma}{d\Omega}. \tag{47}$$

E. Energy-dependent scattering cross-section method

We consider electrons of initial momentum $\vec{q}_1$, entering the irradiated region, containing n_a atoms per cm^3. From Eq. (30), the power absorbed by the electron can be calculated by integrating over all possible directions of the final momentum $\vec{p}_2$

$$d\dot{W}=n_e f(q_1)d^3q_1 n_a\frac{p_1}{m}\int d\Omega_{p_2}\Delta E\frac{d\sigma(\vec{p}_1,\vec{p}_2)}{d\Omega}. \tag{48}$$

The total power absorption is derived by integrating over the initial momenta $\vec{q}_1$, and taking the time average. ΔE is taken from Eq. (28):

$$\dot{W}=n_e n_a\int d^3q_1 f(\vec{q}_1)\int_0^{\pi}\frac{d\alpha}{\pi}\frac{p_1}{m}\int d\Omega_{p_2}\left(\frac{e}{mc}\vec{a}\cdot\vec{Q}\cos\alpha\right)$$
$$\times\frac{d\sigma(\vec{p}_1,\vec{p}_2)}{d\Omega}. \tag{49}$$

We define

$$K\equiv\int_0^{\pi}\frac{d\alpha}{\pi}\frac{p_1}{m}\int d\Omega_{p_2}\left(\frac{e}{mc}\vec{a}\cdot\vec{Q}\cos\alpha\right)\frac{d\sigma(\vec{p}_1,\vec{p}_2)}{d\Omega}. \tag{50}$$

For a beam of electrons with momentum $\vec{q}_1$

$$\dot{W}=n_e n_a K. \tag{51}$$

For convenience, we write Eq. (50) in spherical coordinates

$$\dot{W}=n_e n_a \int_0^{2\pi} d\varphi_0 \int_0^{\pi} d\theta_0 \sin\theta_0 \int_0^{\infty} dq_1 q_1^2 f(q_1,\theta_0,\varphi_0) K , \tag{52}$$

where (θ_0,φ_0) are polar and aximuthal angles of $\vec{q}_1$ relative to the direction of $\vec{a}$, i.e., relative to the direction of polarization of the em wave, and $\cos\theta_0=\hat{a}\cdot\hat{q}_1$. For the calculation of K we also define (θ_1,φ_1) as the angles of $\vec{p}_1$ relative to $\vec{a}$, and $\cos\theta_1=\hat{a}\cdot\hat{p}_1$. (θ,φ) are the angles of $\vec{p}_2$ relative to $\vec{p}_1$, and $\cos\theta=\hat{p}_1\cdot\hat{p}_2$. The integral over $d\Omega_{p_2}$ can be evaluated with $\int d\Omega_{p_2}=\int_0^{2\pi} d\varphi \int_0^{\pi} d\theta \sin\theta$. The cross section can be expressed for elastic collisions as a function of $p_1^2/2m = p_2^2/2m$ and the angle θ between $\vec{p}_1$ and $\vec{p}_2$

$$\frac{d\sigma}{d\Omega}(\vec{p}_1,\vec{p}_2)=\frac{d\sigma(p_1^2/2m,\theta)}{d\Omega} . \tag{53}$$

$\vec{a}\cdot\vec{Q}$ can be expressed as follows:

$$\begin{aligned}\vec{a}\cdot\vec{Q}&=\vec{a}\cdot(\vec{p}_2-\vec{p}_1)=\vec{a}\cdot\vec{p}_2-ap_1\cos\theta_1\\&=ap_1[(\cos\theta-1)\cos\theta_1+\sin\theta\cos\varphi\sin\theta_1] .\end{aligned} \tag{54}$$

Substituting in Eq. (50)

$$\begin{aligned}K&=\left(\frac{ea}{mc}\right)\int_0^{\pi}\frac{d\alpha}{\pi}\frac{p_1^2}{m}\int_0^{2\pi}d\varphi\int_0^{\pi}d\theta\sin\theta\cos\alpha[(\cos\theta-1)\cos\theta_1+\sin\theta\cos\varphi\sin\theta_1]\frac{d\sigma(p_1^2/2m,\theta)}{d\Omega}\\&=-\left(\frac{ea}{mc}\right)\int_0^{\pi}\frac{d\alpha}{\pi}\cos\alpha\frac{p_1^2}{m}\cos\theta_1\sigma_M\left(\frac{p_1^2}{2m}\right),\end{aligned} \tag{55}$$

where $\sigma_M(E)$ is the momentum-transfer cross section defined by

$$\sigma_M(E)\equiv 2\pi\int_0^{\pi}d\theta\sin\theta(1-\cos\theta)\frac{d\sigma(E,\theta)}{d\Omega} . \tag{56}$$

In Eq. (55) p_1 and θ_1 depend on time, i.e., depend on $\alpha\equiv\omega t$, and should be expressed by q_1, θ_0, and φ_0. From Eq. (25) we obtain

$$p_1^2=q_1^2+\left(\frac{e}{c}a\cos\alpha\right)^2-2\frac{e}{c}\vec{a}\cdot\vec{q}_1\cos\alpha , \tag{57}$$

$$q_1^2=p_1^2+\left(\frac{e}{c}a\cos\alpha\right)^2+2\frac{e}{c}\vec{a}\cdot\vec{p}_1\cos\alpha . \tag{58}$$

Therefore,

$$p_1\cos\theta_1=q_1\cos\theta_0-\frac{e}{c}a\cos\alpha . \tag{59}$$

Substituting Eq. (59) into (55):

$$K=-\left(\frac{ea}{mc}\right)\int_0^{\pi}\frac{d\alpha}{\pi}\cos\alpha\left(\frac{q_1}{m}\cos\theta_0-\frac{ea}{mc}\cos\alpha\right)p_1\sigma_M\left(\frac{p_1^2}{2m}\right) . \tag{60}$$

From Eq. (57) we can express p_1 as

$$p_1=(2m)^{1/2}\left[\frac{q_1^2}{2m}+\frac{1}{2m}\left(\frac{e}{c}a\cos\alpha\right)^2-\frac{ea}{mc}q_1\cos\theta_0\cos\alpha\right]^{1/2} . \tag{61}$$

For convenience we define $E=E_1=q_1^2/2m$, and $\Lambda\equiv 2ea/cq_1$. Using these definitions Eq. (61) can be written as

$$p_1=(2mE)^{1/2}(1+\tfrac{1}{4}\Lambda^2\cos^2\alpha-\Lambda\cos\theta_0\cos\alpha)^{1/2} . \tag{62}$$

Then the following expansion around E is made:

$$\begin{aligned}p_1\sigma_M\left(\frac{p_1^2}{2m}\right)=(2m)^{1/2}\Big(&E^{1/2}\sigma_M+(\tfrac{1}{4}\Lambda^2\cos^2\alpha-\Lambda\cos\theta_0\cos\alpha)E\frac{\partial}{\partial E}(E^{1/2}\sigma_M)\\&+\tfrac{1}{2}(\tfrac{1}{4}\Lambda^2\cos^2\alpha-\Lambda\cos\theta_0\cos\alpha)^2E^2\frac{\partial^2}{\partial E^2}(E^{1/2}\sigma_M)+\cdots\Big) .\end{aligned} \tag{63}$$

For $\Lambda\ll 1$ we can neglect powers of Λ higher than one [provided $\sigma_M(E)$ is far from a resonance]. This gives linear dependence of $\dot{W}$ on the intensity of the incident em wave. However, if Λ is close to one, and/or $\sigma_M(E)$ is near a resonance, higher orders of Λ should be kept, thus giving nonlinear dependence of $\dot{W}$ on the incident intensity.

At our experimental conditions the incident em wave intensity is about 10 mW cm^{-2}, which means field intensity of 2 V cm^{-1}, and $\Lambda\simeq 5\times10^{-5}$. Therefore, we keep only the first power of Λ in the expansion. But for the incident intensity close to 10^6 W cm^{-2} (at 70 GHz), Λ is close to one, and the expansion (63) fails.

Keeping only the first power of Λ, Eq. (63) is inserted into Eq. (60), and integration over α

gives the following result:

$$K=\left(\frac{e}{c}a\right)^2\frac{2^{1/2}}{m^{3/2}}\left(\tfrac{1}{2}E^{1/2}\sigma_M+\cos^2\theta_0 E\frac{\partial}{\partial E}(E^{1/2}\sigma_M)\right), \tag{64}$$

and can be written also

$$K=\left(\frac{e}{c}a\right)^2\frac{(2E)^{1/2}}{m^{3/2}}\left(\tfrac{1}{2}(1+\cos^2\theta_0)\sigma_M+\cos^2\theta_0 E\frac{\partial\sigma_M}{\partial E}\right). \tag{65}$$

For a single electron, colliding with a single atom, we can compute the average number of photons $\bar{\nu}$ transferred during a scattering event. We divide K of Eq. (65) by the incident electron flux $m^{-1/2}(2E)^{1/2}$, divide by the energy of a photon $\hbar\omega$, and replace ea/c by $e\epsilon/\omega$ where ϵ is the magnitude of the electric field of the incident em wave. The result is

$$\bar{\nu}\sigma_T=\frac{m\omega}{\hbar}\left(\frac{e\epsilon}{m\omega^2}\right)^2\left(\tfrac{1}{2}(1+\cos^2\theta_0)\sigma_M+\cos^2\theta_0 E\frac{\partial\sigma_M}{\partial E}\right), \tag{66}$$

σ_T is the total cross section (for all ν and directions of final momenta $\vec{p}_2$). This result was derived quantum mechanically by Mittleman[31] [his Eq. (2.10)], using the equation derived by Kroll and Watson[27] [Eq. (20) in the present paper]. (In Mittleman's work, $\vec{\alpha}_0\equiv\vec{\epsilon}/m\omega^2$, $\hat{p}_i\cdot\hat{\alpha}_0\equiv\cos\theta_0$, and $\hbar=1$.)

In order to get an estimate of $\bar{\nu}$ at our experimental conditions we take, as an example, incident intensity of 10 mW cm^{-2}, $\epsilon\simeq 2$ V cm^{-1}. We consider an electron of energy $E=25$ eV, incident parallel to the electric field ($\cos^2\theta_0=1$). The calculations of Eq. (66) yield $\bar{\nu}\simeq -0.4\times10^{-4}$. For comparison, calculations were made with Eq. (20). At the above conditions, the argument of the Bessel function is about ten and therefore the probability for absorbing or emitting ν photons during one collision is high for $-10\lesssim\nu\lesssim 10$. This result means that although an order of ten photons are exchanged in a single collision, the average photon exchange is about 5 orders of magnitude smaller. However, as shown in subsection H, this extremely small asymmetry between emission and absorption of photons leads to amplification of significant magnitude.

F. Isotropic distribution

Both methods can be used to calculate a simple expression for isotropic distributions. For such distributions $f(\vec{q})=f(q)=f(E)$ and the normalization is

$$4\pi\int_0^\infty dq\, q^2 f(q)=1\,. \tag{67}$$

We define $F(E)$ so that

$$f(E)=(2\pi)^{-1}(2m)^{-3/2}E^{-1/2}F(E)\,, \tag{68}$$

and $F(E)$ normalized by

$$\int_0^\infty dE\,F(E)=1\,. \tag{69}$$

We define (θ_2,ϕ_2) as the angles of $\vec{q}_2$ relative to $\vec{q}_1$.

Using the method of subsection D, and substituting these definitions in Eq. (40) we obtain

$$\dot{W}=\frac{n_e n_a}{m^{1/2}2^{3/2}(2\pi)}\int_0^\pi\frac{d\alpha}{\pi}\int_0^{2\pi}d\varphi_0\int_0^\pi d\theta_0\sin\theta_0\int_0^{2\pi}d\varphi_2\int_0^\pi d\theta_2\sin\theta_2$$
$$\times\int_0^\infty dE_1\int_0^\infty dE_2(E_1E_2)^{1/2}[E_1^{-1/2}F(E_1)-E_2^{-1/2}F(E_2)]\frac{d\sigma(\vec{p}_1,\vec{p}_2)}{d\Omega}\left(\frac{e}{mc}\vec{a}\cdot\vec{Q}\cos\alpha\right)\delta\left(E_2-E_1-\frac{e}{mc}\vec{a}\cdot\vec{Q}\cos\alpha\right). \tag{70}$$

The integral over φ_0 is immediate. For the integration over E_1 and E_2 the following variables are defined:

$$E\equiv(E_1+E_2)/2,\quad \mathcal{E}=E_2-E_1\,,$$

so that $dE_1dE_2=dE\,d\mathcal{E}$, and $\int_0^\infty dE_1\int_0^\infty dE_2$ transform to $\int_{-\infty}^{+\infty}d\mathcal{E}\int_0^\infty dE$. Since $|E_2-E_1|<E_2,E_1$, also $|\mathcal{E}|<E$, the following approximations can be made:

(1) $(E_1E_2)^{1/2}\cong E$.

(2) The square brackets in (70) can be expanded around E

$$[E_1^{-1/2}F(E_1)-E_2^{-1/2}F(E_2)]\cong-\mathcal{E}\frac{\partial}{\partial E}[E^{-1/2}F(E)]\,.$$

(3) $d\sigma/d\Omega$ will be evaluated at $E\cong p_1^2/2m$ and at scattering angle θ_2, although it is the angle between $\vec{q}_2$ and $\vec{q}_1$ and not between $\vec{p}_2$ and $\vec{p}_1$.

With these approximations Eq. (70) becomes

$$\dot{W}=\frac{n_e n_a}{m^{1/2}2^{3/2}}\int_0^{\pi}\frac{d\alpha}{\pi}\int_0^{\pi}d\theta_0\sin\theta_0\int_0^{2\pi}d\varphi_2\int_0^{\pi}d\theta_2\sin\theta_2\int_0^{\infty}dE\int_{-\infty}^{+\infty}d\mathcal{E}$$
$$\times E\left(-\mathcal{E}\frac{\partial}{\partial E}[E^{-1/2}F(E)]\right)\left(\frac{e}{mc}\vec{a}\cdot\vec{Q}\cos\alpha\right)$$
$$\times\frac{d\sigma(E,\theta_2)}{d\Omega}\delta\left(\mathcal{E}-\frac{e}{mc}\vec{a}\cdot\vec{Q}\cos\alpha\right). \tag{71}$$

The integral over $\mathcal{E}$ is immediate by the δ function; then the integral over α can be evaluated and the $\vec{a}\cdot\vec{Q}$ term can be expressed as

$$\vec{a}\cdot\vec{Q}=\vec{a}\cdot(\vec{q}_2-\vec{q}_1)=aq_2(\cos\theta_2\cos\theta_0+\sin\theta_2\cos\varphi_2\sin\theta_0)-aq_1\cos\theta_0$$
$$\cong a(2mE)^{1/2}[(\cos\theta_2-1)\cos\theta_0+\sin\theta_2\cos\varphi_2\sin\theta_0], \tag{72}$$

where in the last step we assumed $q_1\cong q_2\cong(2mE)^{1/2}$. Substituting (72) into (71) and integrating over the angles we arrive at the expression

$$\dot{W}=-n_e n_a\frac{2^{1/2}}{m^{3/2}}\left(\frac{e}{c}a\right)^2\tfrac{1}{3}\int_0^{\infty}dE\,\sigma_M(E)E^2\frac{\partial}{\partial E}[E^{-1/2}F(E)], \tag{73}$$

where $\sigma_M(E)$ was defined in Eq. (56).

An expression for the isotropic distribution can be derived also in the energy-dependent-cross-section method. We combine Eq. (52) with Eq. (73) and substitute definition (68), so that

$$\dot{W}=n_e n_a\frac{2^{1/2}}{m^{3/2}}\left(\frac{e}{c}a\right)^2\int_0^{2\pi}d\varphi_0\int_0^{\pi}d\theta_0\sin\theta_0\int_0^{\infty}dE\,m(2mE)^{1/2}$$
$$\times\left(\frac{F(E)}{(2\pi)(2m)^{3/2}E^{1/2}}\right)\left(\tfrac{1}{2}E^{1/2}\sigma_M+\cos^2\theta_0 E\frac{\partial}{\partial E}(E^{1/2}\sigma_M)\right). \tag{74}$$

The integrations in Eq. (74) are immediate, and the result is

$$\dot{W}=n_e n_a\frac{2^{1/2}}{m^{3/2}}\left(\frac{e}{c}a\right)^2$$
$$\times\int_0^{\infty}dE\,F(E)\left(\tfrac{1}{2}E^{1/2}\sigma_M+\tfrac{1}{3}E\frac{\partial}{\partial E}(E^{1/2}\sigma_M)\right). \tag{75}$$

This result can be written also in the form

$$\dot{W}=n_e n_a\frac{2^{1/2}}{m^{3/2}}\left(\frac{e}{c}a\right)^2\frac{1}{3}$$
$$\times\tfrac{1}{3}\int_0^{\infty}dE\,F(E)\left(\tfrac{1}{2}E^{1/2}\sigma_M+\frac{\partial}{\partial E}(E^{3/2}\sigma_M)\right), \tag{76}$$

and for comparison we write Eq. (73) in the form

$$\dot{W}=n_e n_a\frac{2^{1/2}}{m^{3/2}}\left(\frac{e}{c}a\right)^2$$
$$\times\tfrac{1}{3}\int_0^{\infty}dE\left(\tfrac{1}{2}E^{1/2}\sigma_M F(E)-E^{3/2}\sigma_M\frac{\partial F(E)}{\partial E}\right). \tag{77}$$

Equation (77) is identical to Eq. (76) since integration by parts yields

$$\int_0^{\infty}dE\,E^{3/2}\sigma_M\frac{\partial F}{\partial E}=E^{3/2}\sigma_M F\Big|_0^{\infty}-\int_0^{\infty}dE\,F\frac{\partial}{\partial E}(E^{3/2}\sigma_M)$$
$$=-\int_0^{\infty}dE\,F\frac{\partial}{\partial E}(E^{3/2}\sigma_M).$$

The last step follows since at $E=\infty$ both $F(E)$ and $\sigma_M(E)$ vanish, and they are finite for $E=0$. Naturally the methods of subsections D and E lead to the same results for the case of isotropic distributions, as the two methods are essentially equivalent.

G. Amplification

When the power absorbed in a unit volume $\dot{W}$ is negative, energy is transferred from the plasma to the electromagnetic wave which is amplified. Assuming an electromagnetic wave of initial power P_0 incident on a plasma cross section S and traveling a distance L in the plasma, it goes out of the plasma with power $P_0-\dot{W}SL$.

The amplification factor is defined by

$$h\equiv\frac{-\dot{W}SL}{P_0}. \tag{78}$$

Simple calculations show that

$$h=-8\pi e^2c^{-1}\omega^{-2}\left(\frac{e}{c}a\right)^{-2}L\dot{W}. \tag{79}$$

Combining Eq. (79) with any equation for $\dot{W}$ in this section gives the amplification h, independent of the incident power, as was found experimentally.

The amplification (or absorption) can be calculated in both methods, either from Eq. (40) based on difference of population method, or from Eqs. (52) and (64) based on the energy dependence of the scattering cross section. The difference of population method is more convenient when the electron distribution is smooth and sufficiently known, but the scattering cross section varies "wildly" or is not known with enough accuracy. The second method is more convenient for sharp electron distributions, such as beams, and when the energy dependence of the scattering cross section is known.

The conditions for amplification can be demonstrated for the case of isotropic distributions as described in Fig. 12. The full line describes a distribution function $E^{-1/2}F(E)$, with a maximum at E_{max}. The dashed line is a momentum-transfer cross section which decreases with energy. According to Eq. (73), negative contribution to $\dot{W}$ arises for $E < E_{max}$ where $\partial/\partial E[E^{-1/2}F(E)] > 0$, and positive contribution for $E > E_{max}$ where $\partial/\partial E[E^{-1/2}F(E)] < 0$. If $\sigma_M(E)$ decreases fast enough with energy, the negative contribution outweighs the positive one and the em wave is amplified. As an intuitive criterion for amplification, one may say that the maximum of the distribution function should be in the region where $\sigma_M(E)$ decreases strongly with energy. Since for low energies most scattering cross sections are nearly independent of energy, or even increasing with energy, no amplification can be achieved with Maxwellian distributions. Alternatively, from Eq. (75) the condition for amplification for an isotropic distribution is given by

$$\left(\tfrac{1}{2}E^{1/2}\sigma_M + \tfrac{1}{3}E\frac{\partial}{\partial E}(E^{1/2}\sigma_M)\right) = \tfrac{1}{3}E^{1/2}\left(2\sigma_M + E\frac{\partial\sigma_M}{\partial E}\right) < 0 . \quad (80)$$

Again, the criterion for amplification is that most of the electrons are with energy in the range where $\sigma_M(E)$ decreases fast enough so that $-E\partial\sigma_M/\partial E > 2\sigma_M$.

For anisotropic distributions, the amplification depends on the direction of the polarization relative to the preferred direction of the distribution. This can be seen in Eq. (40), and Eqs. (46) and (47). But it is more instructive to examine Eq. (64). For a beam of electrons of energy E, incident with an angle θ_0 relative to the polarization direction, the amplification is proportional to

$$\tfrac{1}{2}E^{1/2}\sigma_M + \cos^2\theta_0 E\frac{\partial}{\partial E}(E^{1/2}\sigma_M)$$

Since $(E\partial/\partial E)(E^{1/2}\sigma_M)$ is the term contributing to amplification (when it is negative), the greater $\cos^2\theta_0$, the greater the amplification. Therefore, maximum amplification is achieved for a beam parallel to the polarization ($\cos^2\theta_0 = 1$), and absorption follows from a beam perpendicular to the polarization direction ($\cos^2\theta_0 = 0$).

The amplification can be explained in a simple way: An electron of initial energy E is periodically (in time) accelerated and decelerated by the incident em wave, so that energy is transferred periodically from the em wave to the electron and back from the electron to the em wave. A collision process of an electron which loses energy to the field contributes to amplification, and vice versa. The periods of acceleration and deceleration are equal, but if the collision cross section decreases with energy, the electron which loses energy to the field has a greater probability of making a collision than the one which gains energy from the field, so that amplification outweighs absorption. However, the flux of the electrons which lose energy is lower than of those which gain energy, and this reduces the amplification. The real situation is more complicated due to the geometry of the collision process.

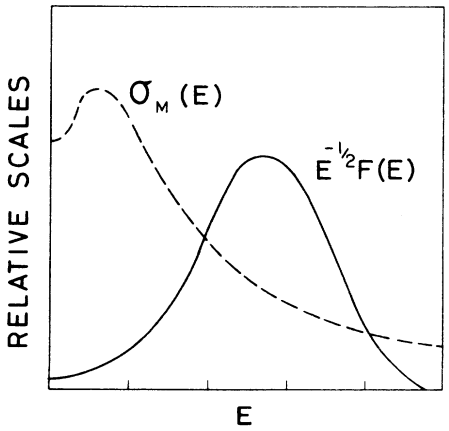

FIG. 12. Schematic diagram for demonstrating the conditions for amplification. Full line: electron distribution $E^{-1/2}F(E)$ versus the energy E. Dashed line: momentum-transfer cross section σ_M versus the electron energy E.

H. Evaluation of the amplification

It is more convenient to evaluate the amplification with the expressions derived in the method based on the energy dependence of the collision cross section. We calculated the amplification for two extreme cases: (I) A beam of electrons with energy E directed in the direction of polarization of the electromagnetic wave. (II) Isotropic distribution of electrons with energy E. In case (I)

the amplification is derived from Eqs. (51), (65), and (79):

$$h = -\frac{8\pi e^2}{c\omega^2 m^{3/2}} L n_e n_a (2E)^{1/2} \times \left(\tfrac{1}{2}(1+\cos^2\theta_0)\sigma_M + \cos^2\theta_0 E \frac{\partial\sigma_M}{\partial E}\right), \quad (81)$$

where $\cos^2\theta_0 = 1$, so the expression in parentheses becomes $(\sigma_M + E\partial\sigma_M/\partial E)$. In case (II), the amplification is derived from Eqs. (75) and (79),

$$h = -\frac{8\pi e^2}{c\omega^2 m^{3/2}} L n_e n_a \left(\frac{2}{3}\right)^{1/2} \times \int_0^\infty dE\, F(E) E^{1/2} \left(2\sigma_M + E\frac{\partial\sigma_M}{\partial E}\right), \quad (82)$$

where we assume $F(E') = \delta(E - E')$, so that we get an expression

$$h = -\frac{8\pi e^2}{c\omega^2 m^{3/2}} L n_e n_a (2E)^{1/2} \tfrac{1}{3} \left(2\sigma_M + E\frac{\partial\sigma_M}{\partial E}\right). \quad (83)$$

Values of $\sigma_M(E)$ for energies above 20 eV with sufficient accuracy to calculate $\partial\sigma_M/\partial E$ are needed. We found such values for He.[32] The pressure was taken as 1.0 mm Hg so that $n_a \cong 3\times10^{16}$ cm^{-3}, $\omega = 2\pi\times70\times10^9$ Hz, and $L = 2$ cm. We made the calculations for $n_e = 10^{13}$ cm^{-3}. The results for $E = 25$, 50, 100, and 200 eV, are given in Table I. h was expressed as percents. Negative values indicate absorption.

As can be seen from Table I, small amplification can be achieved even for isotropic distributions, if most electrons have energy above 100 eV. In the case of an optimally directed beam the amplification is stronger at energies close to 25 eV.

The cathode region of a cold-cathode glow discharge is characterized by high electron density with special distributions. The density of electrons can be estimated from the refraction measurements of Sec. IV. As was shown there, for the refraction to be significant n_e must be close to $n^0 = 6\times10^{13}$ cm^{-3}. Since we found significant divergence of the em wave n_e must be of the order of 10^{13} cm^{-3}, which was used in our calculations. The distribution of the electrons is not well known. Measurements were made by Volkova *et al.*[33] in a hot-cathode discharge. They found that the distribution in the negative glow was "inverted," with a maximum at an energy of 30 eV, which is about half of the cathode fall voltage, which was 60 V. The condition of their experiments are quite similar to ours, but since the cathode was hot the cathode fall voltage was much lower. At our conditions the cathode fall voltage was about 400 V, therefore, we expect the maximum of electron distribution to be at about 200 eV. The distribution is assumed to be slightly anisotropic.

TABLE I. Calculated values of amplification h (in percent) of Eqs. (81) and (83) for several electron energies E, and electron density 10^{13} cm^{-3}. Negative values indicate absorption. Scattering gas: He, at 1-mm Hg pressure.

E (eV)	Amplification h (%) Beam	Isotropic
25	1.4	−0.8
50	1.3	−0.2
100	0.9	0.01
200	0.6	0.07

The calculations, based on the assumed properties of the negative glow at our experimental conditions, yield amplification of about 1%, which is of the right order of magnitude, but somewhat lower than the measured values. It should be noted that the derivation of the theoretical expressions relies on some assumptions which are not accurate. We shall indicate some of the possible improvements of the theory.

(1) Inelastic collisions should be included in the calculations, and other possible collisions, for example, collisions with ions.

(2) The effect of finite atom mass should be considered.

(3) The em wave was assumed to be a plane wave, but the real wave in our experiments was concentrated by a lens to a region comparable to the wavelength. The effect of this concentration should be investigated.

(4) The incident em wave might change the electron distribution and create some "bunching" which should intensify the amplification.

(5) The incident em wave affects the scattering atom so that $d\sigma/d\Omega$ is changed. This effect may be small, but important for amplification processes.

[1]A. Rosenberg, J. Felsteiner, Y. Ben-Aryeh, and J. Politch, Phys. Rev. Lett. 45, 1787 (1980).
[2]G. B. Burrough and A. Bronwell, Tele-Tech. 11, 62 (1952).
[3]P. J. W. Severin, Philips Res. Rep. Suppl. 2 (1965).
[4]N. S. Kopeika and N. H. Farhat, IEEE Trans. Electron Devices ED-22, 534 (1975) (Part I); ED-22, 540 (1975) (Part II); ED-23, 1113 (1976).

[5]M. A. Lampert and A. D. White, Electr. Commun. 30, 124 (1953).
[6]B. Udelson, J. Appl. Phys. 28, 380 (1957).
[7]J. Bloyet and A. Talsky, C. R. Acad. Sci. B270, 448 (1970).
[8]R. L. Taylor and S. B. Herskovitz, Proc. IRE 49, 1901 (1961).
[9]R. A. Demirkhanov, A. K. Gevorkov, A. F. Popov, and G. L. Khorasanov, Radiotekh. Elektron. 8, 1489 (1963) [Radio Eng. Electron. Phys. (USSR) 8, 1433 (1963)].
[10]G. D. Lobov and V. I. Eremeyev, Radiotekh. Elektron. 6, 286 (1961) [Radio Eng. Electron. (USSR) 6, 152 (1961)].
[11]G. D. Lobov, Radiotekh. Elektron. 5, 1848 (1960) [Radio Eng. Electron. (USSR) 5, 152 (1960)].
[12]K. I. Kononenko, Izv. Vyssh. Uchebn. Zaved. Radiofiz. 8, 972 (1965) [Sov. Radio Phys. 8, 696 (1965)].
[13]A. Von Engel, *Ionized Gases*, 2nd ed. (Oxford, Clarendon, 1965).
[14]L. Goldstein, J. M. Anderson, and G. L. Clark, Phys. Rev. 90, 486 (1953).
[15]J. M. Anderson, Phys. Rev. 108, 898 (1957).
[16]C. L. Chen, C. C. Leiby, and L. Goldstein, Phys. Rev. 121, 1391 (1961).
[17]R. Opher, J. Politch, and J. Felsteiner, Appl. Phys. Lett. 32, 701 (1978).
[18]A. Rosenberg, J. Politch, J. Felsteiner, and R. Opher, J. Phys. D 13, 813 (1980).
[19]A. Weingartshofer, J. K. Holmes, G. Caudle, E. M. Clarke, and H. Kruger, Phys. Rev. Lett. 39, 269 (1977).
[20]A. Weingartshofer, E. M. Clarke, J. K. Holmes, and C. Jung, Phys. Rev. A 19, 2371 (1979).
[21]F. F. Chen, *Introduction to Plasma Physics* (Plenum, New York, 1974), pp. 100–107.
[22]J. Politch and N. H. Farhat, J. Phys. E 11, 623 (1978).
[23]N. H. Farhat and J. Politch, J. Phys. E 12, 89 (1979).
[24]D. Marcuse, Bell Syst. Tech. J. 41, 1557 (1962).
[25]F. B. Bunkin, A. E. Kazakov, and M. V. Fedorov, Usp. Fiz. Nauk 107, 559 (1972) [Sov. Phys.—Usp. 15, 416 (1973)].
[26]M. V. Fedorov, Izv. Akad. Nauk SSSR, Ser. Fiz. 42, 2473 (1978) [Bull. Acad. Sci. USSR, Phys. Ser. 42, 12 (1978)].
[27]N. M. Kroll and K. M. Watson, Phys. Rev. A 8, 804 (1973).
[28]M. Gavrila and M. Van der Wiel, Comments At. Mol. Phys. 8, 1 (1978).
[29]G. Ferrante, Phys. Rev. A 22, 2529 (1980).
[30]L. Schlessinger and J. Wright, Phys. Rev. A 20, 1934 (1979).
[31]M. H. Mittleman, Phys. Rev. A 21, 79 (1980).
[32]D. F. Register, S. Trajmar, and S. K. Srivastava, Phys. Rev. A 21, 1134 (1980).
[33]L. M. Volkova, A. M. Devyatov, E. A. Kralkina, and A. V. Kuralova, J. Phys. (Paris) Colloq. Suppl. 7, 40, C7-231 (1979).